HIGH-STRENGTH AL-BASED ALLOYS WITH NANOGRANULAR AMORPHOUS AND FCC-AL PHASES

Hisamichi KIMURA, Kenichiro SASAMORI and Akihisa INOUE

Institute for Materials Research, Tohoku University, Sendai 980-8577, Japan

ABSTRACT A new nanogranular structure consisting of amorphous and fcc-Al phases was formed in melt-spun Al-V-Fe, Al-V-Co, Al-Ti-Fe, Al-Ti-Co and Al-Ti-Ni alloys. The nanogranular amorphous phase crystallizes to an icosahedral phase at about 623 K for the Al-4at%V-2at%Fe ($Al_{94}V_4Fe_2$) alloy and to Al_3Ti phase at about 673 K for the Al-5at%Ti-2at%Fe ($Al_{93}Ti_5Fe_2$) alloy. The nanogranular alloys exhibit good bending ductility and high mechanical strength with tensile strength (σ_f) of 1390 MPa and Vickers hardness (H_v) of 470 for $Al_{94}V_4Fe_2$ alloy, 1210 MPa and 440 for $Al_{93}Ti_5Fe_2$ alloy and 1320 MPa and 440 for $Al_{93}Ti_4Fe_3$ alloy. The high σ_f above 1000 MPa is retained in the temperature up to 500 K. The amorphous phase decomposes around 600 K, accoMPanying the decrease in σ_f and the increase in elongation. The formation of the nanogranular amorphous phase at the Al-rich compositions between 92 and 94 at%Al is important for future development of a new type of Al-based alloys with high specific mechanical strength.

Keywords: aluminum base alloy, amorphous phase, mechanical strength, elevated-temperature strength, oxidation

1. INTRODUCTION

Bulk nanocrystalline alloys in Al-Ni-Zr-Mm (Mm=misch metal) system prepared by extrusion atomized amorphous powders have attracted great attention because of the simultaneous achievements of high tensile strength, high fatigue strength, high elevated tempeture strength and high stiffness [1-3] . It has subsequently been reported that the extrusion of nanoscale quasicrystalline base powders in Al-Mn-Co-Ni, Al-Mn-Co-Ni-Ln (Ln=lanthanide metal), Al-Mn-TM (TM=transition metal), Al-Cr-TM, Al-Cr-Ce-TM and Al-V-Fe systems also causes the production of high-strength Al base alloys with nanoscale icosahedral plus fcc-Al phases [4-10] . This paper aims to examine the composition ranges in which a new type of high-strength bulk alloy containing nanogranular amorphous phase is formed in melt-spun Al-V-Fe, Al-V-Co, Al-Ti-Fe, Al-Ti-Co and Al-Ti-Ni alloys and the compositional and temperature dependence of σ_f and H_v for the alloys containing the nanogranular amorphous phase and to investigate the possibility of fabricating a new type of high-strength bulk alloy by the use of extrusion process of the nonequilibrium phase powders.

2. EXPERIMENTAL PROCEDURE

Ternary Al-V-TM (TM=Fe or Co) and Al-Ti-TM(TM=Fe, Co or Ni) alloys were used in the present study. The alloy ingots were prepared by arc melting the mixture of pure Al, V, Ti, Fe, Co and Ni metals in an argon atmosphere. The rapidly solidified alloys were produced by melt spinning in an argon atmosphere. The circumferential velocity was fixed to be 40 m/s. The structure in as-quenched and annealed states was examined dy differential scanning calorimetry (DSC). Tensile strength and elongation were measured by an Instron-type tensile testing machine at a strain rate of 8.3×10^{-4} s^{-1} in the temperature range from room temperature to 723 K and Vickers hardness was measured by a Vickers microhardness tester with a load of 25 g. Oxidation behavior was examined by thermogravimetric analysis (TGA) at a rate of 0.17 K/s in air.

3. RESULTS AND DISCUSSION

3.1 Rapidly solidified structure

Figure 1 shows the X-ray diffraction patterns of the rapidly solidified $Al_{94}V_4Fe_2$ and $Al_{93}Ti_5Fe_2$ alloys. In addition to the diffraction peaks of fcc-Al phase, one can see a broad peak corresponding to the formation of an amorphous phase. It is to be noticed that coxistent amorphous plus fcc-Al phases are formed even at the high Al compositions. In order to clarify the coexistent microstructure, the highly magnified TEM images and selected-area electron patterns of the $Al_{94}V_4Fe_2$ and $Al_{93}Ti_5Fe_2$ alloys are shown in Fig. 2. Although the diffraction patterns reveal the coexistence of amorphous and fcc-Al phases, the microstructure differs

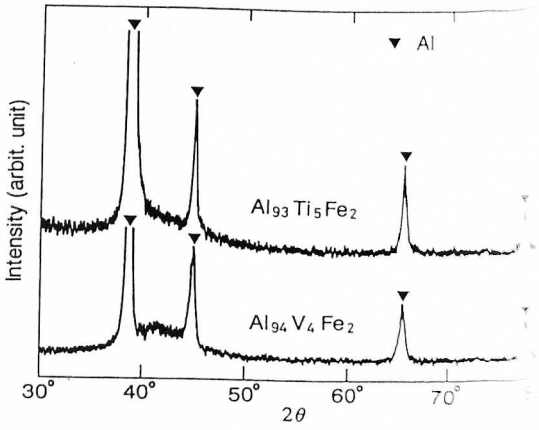

Fig. 1 X-ray diffraction patterns of rapidly solidified $Al_{94}V_4Fe_2$ and $Al_{93}Ti_5Fe_2$ alloys.

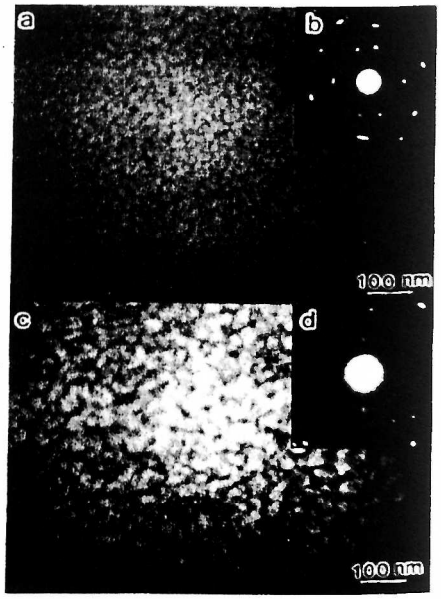

Fig. 2 Bright-field electron micrographs and selected-area electron diffraction patterns of rapidly solidified $Al_{94}V_4Fe_2$ (a and b) and $Al_{93}Ti_5Fe_2$ (c and d) alloys.

significantly between the two alloys. As shown in Fig. 2 (a), the rapidly solidified $Al_{94}V_4Fe_2$ alloy consists of homogeneously mixed granular amorphous and fcc-Al phases. On the other hand, as shown in Fig. 2 (c), the $Al_{93}Ti_5Fe_2$ alloy consists of equiaxed fcc-Al grains embedded in the network of an amorphous phase, being different from that for the $Al_{94}V_4Fe_2$ alloy. The marked difference in the solidification structure takes place through the primary formation of an amorphous phase, followed by the precipitation of fcc-Al phase from the remaining liquid for the Al-V-Fe alloy, while that for the Al-Ti-Fe alloy results from the primary precipitation of fcc-Al phase and then the solidification of the remaining liquid to an amorphous phase.

3.2 Mechanical strength

The tensile fracture strength (σ_f) and Vickers hardness number (H_v) of the $Al_{94}V_4M_2$ (M= Fe or Co) alloys are 1390MPa and 470, respectively, for M=Fe and 1230MPa and 460, respectively, for Co. The fracture surface consists mainly of a unique pattern typical for ductile amorphous alloys, as examplified in Fig. 3. Similarly, the σ_f and H_v for the $Al_{93}Ti_5M_2$ (M=Fe, Co or Ni) alloys are, respectively, 1210MPa and 440 for M=Fe, 1120MPa and 440 for Co and 920MPa and 460 for Ni. The σ_f and H_v for the $Al_{93}Ti_4M_3$ (M=Fe, Co or Ni) alloys are also, respectively, 1320MPa and 450 for M=Fe, 1050MPa and 430 for Co and 1020MPa and 400 for Ni. Thus, these strength values appear to decrease in the order of Fe>Co>Ni. These changes indicate clearly that the good mechanical properties

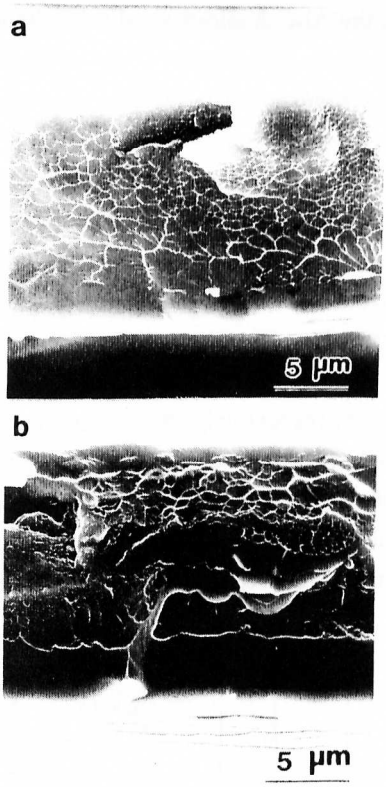

Fig. 3 Scanning electron micrographs revealing the tensile fracture surface appearance of rapidly solidified $Al_{94}V_4Fe_2$ (a) and $Al_{93}Ti_5Fe$ (b) alloys.

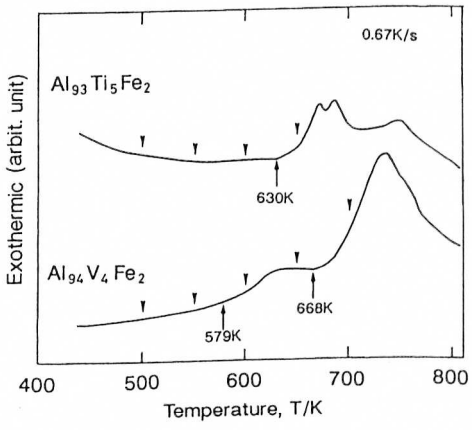

Fig. 4 DSC curves of rapidly solidified $Al_{94}V_4Fe_2$ and $Al_{93}Ti_5Fe_2$ alloys heated in a flowing argon atmosphere.

for the Al-rich alloys are due to the formation of the unique nanostructure.

3.3 Changes in the microstructure and mechanical strength with annealing temperature

It is of importance to examine the thermal stability of the nanogranular amorphous in coexistence with Al phase. Figure 4 shows the DSC curves for the rapidly solidified $Al_{94}V_4Fe_2$ and $Al_{93}Ti_5Fe_2$ alloys, which were measured at the heating rate of 0.67 K/s. It is seen that the onset temperature of crystallization is 579 and 668 K for the former alloy and 630 K for the latter alloy. The X-ray diffraction patterns of the Al-V-Fe and Al-Ti-Fe alloys annealed for 900 s at various temperature marked by arrows on the DSC curves in Fig. 4 are shown in Fig. 5 and Fig. 6, respectively. As indexed in the Fig. 5, the amorphous plus fcc-Al phases remain almost unchanged in the temperature range up to 600 K and change to icosahedral plus fcc-Al phases followed by $Al_{11}V$ plus $Al_{23}V_4$ plus fcc-Al phases. The first and second exothermic reactions are due to the transition from amorphous to icosahedral phase and from icosahedral to crystalline phases, respectively. On the other hand, as indexed in the Fig. 6, the amorphous plus fcc-Al

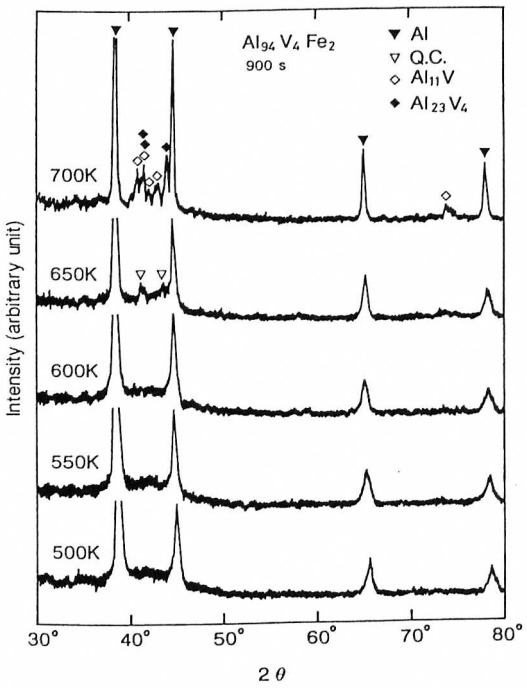

Fig. 5 X-ray diffraction patterns of rapidly solidified $Al_{94}V_4Fe_2$ samples annealed for 900 s at various temperature between 500 K and 700K.

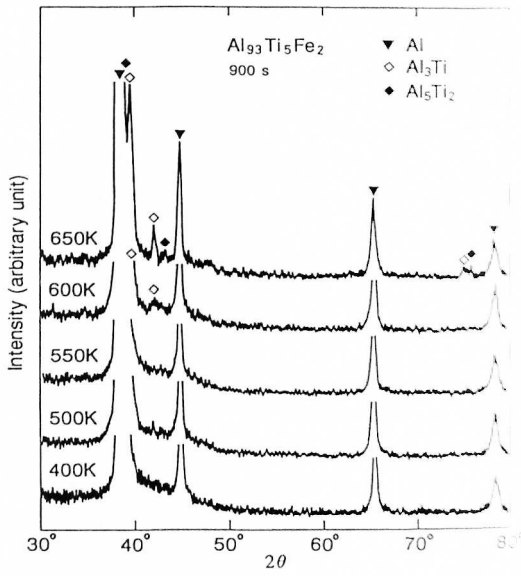

Fig. 6 X-ray diffraction patterns of rapidly solidified $Al_{93}Ti_5Fe_2$ samples annealed for 900 s at various temperature between 400 K and 650K

phases remain almost unchanged in the temperature range up to 550 K and change to Al_3Ti plus fcc-Al phases, followed by Al_3Ti plus Al_5Ti_2 plus fcc-Al phases. Figure 7 shows the nominal tensile stress-elongation curves of the rapidly solidified $Al_{94}V_4Fe_2$ alloy. The σ_f of the $Al_{94}V_4Fe_2$ alloy decreases gradually from 1390 to 620 MPa in the temperature range from room temperature to 680 K. On the other hand, the ε_f increases slightly from 2.6 to 4.3 % at temperature below 640 K and then significantly to 3.9 % with increasing temperature to 680 K. The high values of 900 MPa for σ_f and 4.3 % for ε_f are retained at 640 K and the further increase in testing temperature causes the significant decrease in σ_f to 620 MPa at 680 K and the rapid increase in ε_f to 22 %. The similar high σ_f of 900 MPa at 640 K is also obtained for the $Al_{93}Ti_5Fe_2$ alloy, as shown in Fig. 8. These results allow us to conclude that the Al-V-Fe and Al-Ti-Fe alloys consisting of mixed nanogranular amorphous and fcc-Al phases have high elevated-temperature strength of about 900 MPa at 640 K. The high elevated-temperature strength is consistent with the result that the high mechanical strength above 1000 MPa is retained even after annealing for 900 s at 600 K.

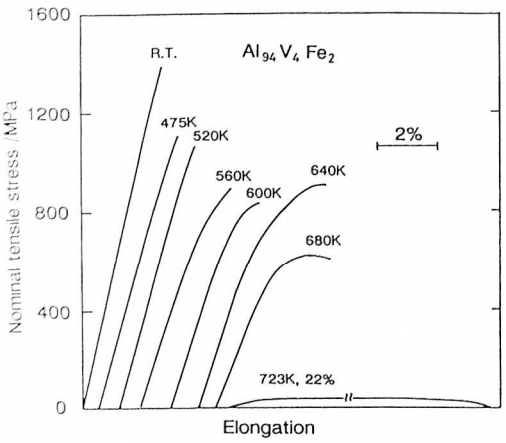

Fig. 7 The temperature dependence of nominal tensile stress-elongation curves of rapidly solidified $Al_{94}V_4Fe_2$ alloy.

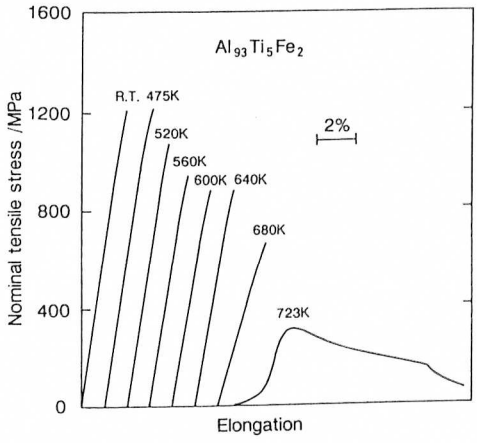

Fig. 8 The temperature dependence of nominal tensile stress-elongation curves of rapidly solidified $Al_{93}Ti_5Fe_2$ alloy.

3.4 Oxidation

Figure 9 shows the TGA curves for the rapidly solidified $Al_{94}V_4Fe_2$ and $Al_{93}Ti_5Fe_2$ alloys in air, where the measurements were done at the heating rate of 0.17 K/s. The data of the pure Al with high resistance for oxidation are also shown for comparison. On heating up to 800 K from room temperature, the increase weight $\triangle W/W$ for the $Al_{93}Ti_5Fe_2$ alloy is nearly the same as that for pure Al, but the $\triangle W/W$ of the $Al_{94}V_4Fe_2$ alloy is about 3 times larger than that of pure Al at

800 K. These results indicate that the $Al_{93}Ti_5Fe_2$ alloy has a high resistance against the elevated-temperature oxidation.

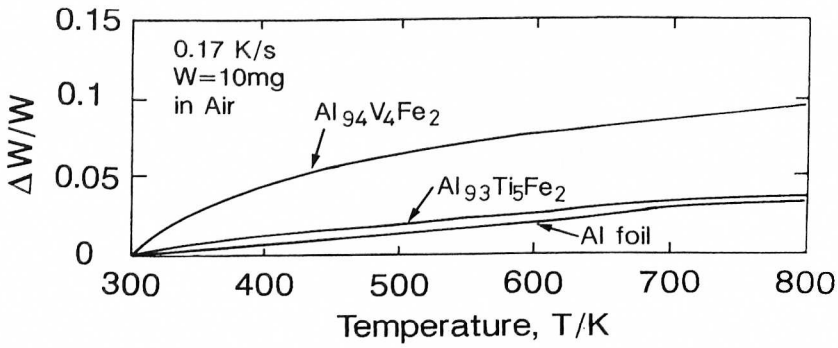

Fig. 9 Temperature variation of rapidly solidified $Al_{94}V_4Fe_2$ and $Al_{93}Ti_5Fe_2$ samples weight in air.

REFERENCES

[1] A. Inoue : Mater. Sci. Eng., A179/A180(1994), 57.

[2] A. Inoue and T. Masumoto : The 3rd Int. Conf. on Aluminum Alloys, ed. L. Arnberg (SINTEF, Trondheim, 1994), p. 45.

[3] K. Ohtera : Doctor Thesis, Tohoku University, (1996).

[4] A. Inoue and H. M. Kimura : Processing and Properties of Nanocrystalline Materials, ed. C. Suryanarayana, J. Singh and F. H. Froes (TMS, Warrendale, 1996), 367.

[5] A. Inoue and H. M. Kimura : Synthesis and Processing of Nanocrystalline Powder, ed. D. L. Bourell (TMS, Warrendale, 1996), p. 91.

[6] K. Kita, T. Saitoh, A. Inoue and T. Masumoto : Mater. Sci. Eng., A226/A228(1997), 1004.

[7] H. M. Kimura, A. Inoue, K. Sasamori and Y. Kawamura : J. Jpn. Soc. Powder & Powder Metallurgy 44(1997), 858.

[8] H. M. Kimura, A. Inoue, K. Sasamori and Y. Kawamura : J. Jpn. Inst. Light Met., 47(1997), 487.

[9] H. M. Kimura, A. Inoue, K. Sasamori and Y. Kawamura : J. Jpn. Inst. Light Met., 47(1997), 539.

[10] H. M. Kimura, A. Inoue, K. Sasamori and Y. Kawamura : J. Jpn. Inst. Light Met., 48(1998), 127.